Sustainable Chemically Modified Mater-Bi/Poly(ε-caprolactone)/Cellulose Biocomposites: Looking at the Bulk through the Surface

Aleksander Hejna (aleksander.hejna@put.poznan.pl)
Poznan University of Technology
Mateusz Barczewski
Poznan University of Technology
Paulina Kosmela
Gdańsk University of Technology
Olga Mysiukiewicz
Poznan University of Technology
Agnieszka Tercjak
University of the Basque Country (UPV/EHU)
Adam Piasecki
Gdańsk University of Technology
Mohammad Reza Saeb
Gdańsk University of Technology
Marek Szostak
Poznan University of Technology

Research Article

Keywords: Mater-Bi, poly(ε-caprolactone), cellulose filler, biocomposites, filler modification, interfacial adhesion

Posted Date: June 16th, 2023

DOI: https://doi.org/10.21203/rs.3.rs-3064683/v1

Abstract

Sustainable polymer composites are progressively under development in a technological paradigm shift from "just use more and more" to "convert into value-added products". The bio-based blends based on Mater-Bi bio-plastic (A) and poly(ε-caprolactone) (B), at a weight ratio of 70:30 (A:B) were developed, followed by the addition of UFC100 cellulose (C) filler to yield 70/30 (w/w) (A:B)/C sustainable biocomposites. The effects of chemical modification of C with three diisocyanates, i.e., hexamethylene diisocyanate (HDI), methylene bisphenyl isocyanate (MDI), or toluene diisocyanate (TDI) on the surface properties of biocomposites was evaluated by water contact angle and surface roughness detected by atomic force microscopy (AFM). Biocomposites containing C modified with HDI, MDI, or TDI revealed contact angle values of 93.5°, 97.7°, and 92.4°, respectively, compared to 88.5° for reference blend, indicating enlarged hydrophobicity window. This action was further approved by increased fracture surface roughness and miscibility detected by microscopic observation (scanning electron microscopy (SEM) and AFM) and in-depth oscillatory rheological evaluation. Correspondingly, thermogravimetric analysis (TGA) and differential scanning calorimetry (DSC) analyses showed more residue and higher melting temperatures for biocomposites, more promisingly with MDI and TDI modifiers. In conclusion, either incorporation or diisocyanate modification of C affects both surface and bulk properties.

1. Introduction

The popularity of biodegradable polymers is progressively increasing over the last years and decades. Lately, their market has been affected by the global pandemic situation and reduced production size in various sectors (Wu 2022). However, the forecasts indicate its rapid growth in the following years, with the compound annual growth rate exceeding even 20% (RameshKumar et al. 2020). Such a development is induced by various law regulations (like European Union Directives) and consumer choices. Considering the sustainability regulations and concerns, including massive pollution with plastic wastes, people are more prone to serve biodegradable materials, especially for packaging and agricultural applications. Nevertheless, despite ever-increasing awareness, inferior performance and high bioplastics costs are still known as the biggest obstacles to increasing their popularity and market share. The results of a survey performed by Brockhaus et al. (Brockhaus et al. 2016) with over thirty plastic product developers indicate that a few customers are willing to pay more for using biodegradable plastics, highlighting the need to enhance their performance and reduce their costs.

Applying fillers is one of the most common methods used in developing low-cost polymer-based materials (DeArmitt and Breese 2001). Proper selection of filler, characterized by the high availability and relatively low price, may show a very beneficial impact on the composites' cost. However, it is essential to select the material, which through its performance and compatibility with polymer matrix, would guarantee satisfactory composite performance. Over the last years, by far, natural and plant-based materials, mostly fibers, have been frequently used as biofillers for the manufacturing of biodegradable polymer composites (Srebrenkoska et al. 2014; Haina et al. 2020; Hejna et al. 2021a). The primary component of all plant-based fibers is cellulose (Abdul Khalil et al. 2017; Shaghaleh et al. 2018; Motaung

and Linganiso 2018; Platnieks et al. 2020). Nevertheless, to be maximally efficient as filler for polymer composites, cellulose fibers, similar to other plant-based materials, often require proper modifications to provide sufficient compatibility with the polymer matrix (Szefer et al. 2018; Liu et al. 2019; Wang et al. 2020; Borrero-López et al. 2021a; Yang et al. 2023). Over the last few years, multiple review works emphasized the need to modify natural fillers for interfacial adhesion enhancement (Mohit and Arul Mozhi Selvan 2018; Ferreira et al. 2019; Hejna et al. 2020a). Due to their chemical structure, mainly high content of hydroxyl groups, the main components of natural fillers, cellulose, hemicellulose, and lignin, offer multiple modification opportunities. Among well-accepted modification methods are silanization, maleation, acetylation, or alkaline treatment, while less popular approaches include esterification, benzoylation, fatty acid, triazine, or isocyanate treatment (Hejna et al. 2020a; Yu et al. 2022). The high content of hydroxyl groups provides isocyanates with the possibility of covalent urethane bonds with a polymer matrix (Barczewski et al. 2021).

In previous work, the impact of cellulose filler modification with isophorone diisocyanate (IPDI), hexamethylene diisocyanate (HDI), toluene diisocyanate (TDI), and methylene diphenyl diisocyanate (MDI) on the mechanical performance of poly(ε-caprolactone) (PCL)-based composites were reported (Hejna and Kosmela 2020). Results indicated that the tensile strength of composite containing 30 wt.% filler almost doubled (from 13.7 to 28.7 MPa) with diisocyanate modification. Likewise, modulus and hardness increased by 25 and 11%, respectively, demonstrating enhanced interfacial interactions resulting from filler modification, which was additionally supported by dynamic mechanical analysis. Similar observations were reported by Xie et al. (Xie et al. 2020), using MDI as a compatibilizer of poly(butylene adipate-co-terephthalate) (PBAT)/bamboo flour composites. They confirmed efficient compatibilization of the studied bioblend by FTIR analysis, pursuing the presence of urethane groups in the biocomposites. As a result, the enhancement of the mechanical performance was significant, such that the incorporation of MDI in 1–4 parts by weight to the system enhanced tensile strength, elongation at break, and impact strength by 74–91%, 191–332%, and 446–664%, respectively.

In light of previous analyses, modification of biofillers with diisocyanate can remarkably enhance biodegradable polymer composites' ultimate properties and performance. Therefore, in the presented work, we investigated the effect of modification of cellulose filler with the most commonly applied diisocyanates of HDI, MDI, and TDI on either the surface or bulk properties of a fully biodegradable polymer blend based on commercially available Mater-Bi NF803 and PCL as parent components. Surface properties are quantified by contact angle and atomic force microscopy (AFM), while scanning electron microscopy (SEM), differential scanning calorimetry (DSC), thermogravimetric analysis (TGA), Fourier-transform infrared (FTIR) spectroscopy, and rheological analyses were used to probe into bulk properties. The above-mentioned works point to the beneficial impact of diisocyanates on PBAT- and PCL-based composites. Considering the chemical composition, thermoplastic starch should also be a promising candidate for applying diisocyanates as composites' compatibilizers.

2. Experimental

2.1. Materials

The commercial starch-based biomaterial Mater-Bi NF803 from Novamont SPA (Novara, Italy) was applied as the matrix for prepared composites. According to the producer, it was characterized by a melt flow index (MFI) of 3.5 g/10 min (150°C/5 kg) and a melting temperature of 110°C.

The poly(ε-caprolactone) Capa 6500 from Perstorp (Malmö, Sweden) was applied as a second component of the polymer matrix. It was characterized by the M_w = 80,000 g/mol, MFI of 7.0 g/10 min (170°C/2.16 kg), and melting temperature of 58–60°C. The introduction of PCL into polymer matrix was driven by its superior performance compared to the as-received Mater-Bi material, which often limits its application range (Haque et al. 2011; Borchani et al. 2019; Hejna 2020; Hejna et al. 2022)

Commercially available cellulose Arbocel® UFC100 from JRS J. Rettenmaier & Söhne GmbH (Germany) was used as filler for polymer composites. It was characterized by an average particle length of 8 μm, an aspect ratio of 4, a bulk density of 160 g/l, and a moisture content of 4.84 wt.%. Figure 1 presents the micrograph of UFC100 cellulose filler obtained with scanning electron microscopy (SEM).

Three different isocyanates were employed as modifiers of cellulose fillers: hexamethylene diisocyanate, methylene diphenyl diisocyanate, and toluene diisocyanate, which were acquired from Sigma Aldrich (Poland). The purity of HDI and MDI was 98%, while for TDI mixture of 2,4-TDI and 2,6-TDI in the 80/20 ratio was used.

2.2. Modifications of UFC100 filler

Prior to its incorporation into the polymer matrix, cellulose filler was subjected to chemical treatment, which was described in detail in previous works (Hejna et al. 2021d, c). The modification was performed using GMF 106/2 Brabender batch mixer at room temperature (varied from 21.1 to 23.1°C) with a rotor speed of 100 rpm. The proper amount of filler was placed in an internal mixer with a calculated amount of diisocyanate (10 wt.%), respectively, to the mass of the filler. Mixing was performed for 5 min, and samples were put in hermetic storage bags. Figure 2 presents schematically the chemical interactions occurring between cellulose filler and diisocyanates during modification leading to the generation of isocyanate or amine groups on the filler surface due to the reaction between isocyanate groups and moisture.

2.3. Preparation of polymer composites

Composites were prepared using GMF 106/2 Brabender batch mixer at 140°C and a rotor speed of 100 rpm. The processing time equaled 6 min, including the 1-min phase of matrix plasticization and 5 min of melt blending with selected filler. Mater-Bi and PCL blended in a 70:30 ratio were applied as the matrix. The filler content in each sample was fixed at 30 wt.%. Figure 3 presents the scheme of the potential interfacial interactions between modified cellulose fillers and components of the polymer matrix. Prepared composites were compression molded at 150°C and 4.9 MPa for 1 min and then kept under

pressure at room temperature for another 5 min to enable solidification of the material. Obtained samples were coded as Blend, UFC100, HDI, MDI, and TDI.

2.4. Characterization

The chemical structure of composites was determined using Fourier transform infrared spectroscopy (FTIR) analysis performed by a Nicolet Spectrometer IR200 from Thermo Fisher Scientific (USA). The device had an ATR attachment with a diamond crystal. Measurements were performed with 1 cm^{-1} resolution in the range from 4000 to 400 cm^{-1} and 64 scans.

Surface wettability was studied through static water contact angle measurements using an Ossila L2004 contact angle goniometer (Ossila Ltd., Sheffield, UK) equipped with a camera and Ossila Contact Angle software. Ten contact angle measurements were taken in random positions, putting drops of ~ 1 µL distiller water onto the surface of the samples with the aid of a syringe. The average values of at least seven measurements were calculated and reported.

The thermal properties of the samples were measured by differential scanning calorimetry (DSC) carried out on a DSC 214 apparatus from Netzsch (Germany). Measurements were performed in the temperature range of -80 to 170°C under a nitrogen atmosphere (30 ml/min gas flow) at a heating/cooling rate of 15°C/min. The heating was performed twice to erase the thermal history of the samples.

The thermal stability of materials was determined by thermogravimetric analysis (TGA) with the temperature set between 35°C and 800°C at a heating rate of 15°C/min under a nitrogen flow using a TG 209 F1 Netzsch apparatus. Samples of 10.0 ± 0.1 mg and ceramic pans were applied.

Rheological investigations were carried out using an Anton Paar MCR 301 rotational rheometer, with 25 mm diameter parallel plates and a 0.5 mm gap under the oscillatory mode. The experiments were conducted at 170°C. The strain sweep experiments were conducted before performing the dynamic oscillatory measurements in the frequency sweep mode. The strain sweep experiments of all the samples were performed at 170°C with a constant angular frequency of 10 rad/s in the varying strain window 0.001–100%. The preliminary investigations allow to determine the value of 0.05% strain as applicable for frequency sweep experiments and located for all samples in the linear viscoelastic (LVE) region for all samples. The angular frequency used during the studies was in the range of 0.05–500 rad/s.

The scanning electron microscope (SEM) Tescan MIRA3 (Brno, Czech Republic) was used to analyze the ırittle fracture surfaces of prepared samples. The accelerating voltage of 12 kV was applied, and a ⁄orking distance of 19 mm. A thin carbon coating with a thickness of approximately 20 nm was eposited on samples using the Jeol JEE 4B vacuum evaporator.

ıtomic force microscopy (AFM) was used to study the morphology of the prepared materials. The quipment used was a scanning probe microscope (SPM) (NanoScope IIIa Multimode from Digital ıstruments, Veeco Instruments Inc., Santa Barbara, CA, USA) in tapping mode (TM-AFM). One beam antilever (125 mm) with a silicon probe (curvature nominal radius of 5–10 nm) was used. Samples were

cut using an ultramicrotome Leica Ultracut R with a diamond blade, and the cross-section of each prepared material were analyzed.

3. Results and discussion

Figure 4 presents the FTIR spectra of analyzed materials and provides insights into their chemical structure. The appearance of obtained spectra is similar to those reported for Mater-Bi by other researchers (Elfehri Borchani et al. 2015; Ruggero et al. 2020). The presence of a broad peak between 3000 and 3600 cm^{-1} can be attributed to the stretching vibrations of hydroxyl groups commonly present in the starch structure, as well as in the cellulose filler (Salmén and Bergström 2009). The appearance of additional sharper signals around 3186 and 3393 cm^{-1} was associated with N-H bonds' vibrations resulting from the cellulose filler modification with isocyanates. Applied treatment resulted in chemical reactions between free isocyanate groups and functional groups (mainly hydroxyl) present on the surface of cellulose particles, which yielded urethane bonds (Barczewski et al. 2021). Moreover, shifts in peak positions could be related to the enhanced hydrogen bonding of O-H and N-H groups within the system resulting from the generation of urethane moieties (Wang et al. 1994). Signals at 2847 and 2917 cm^{-1} were related to the symmetric and asymmetric stretching C-H vibrations. A strong signal was noted at 1720 cm^{-1}, attributed to the vibrations of C = O bonds in the ester groups of PBAT and PCL (França et al. 2019). The introduction of isocyanate-modified fillers resulted in the appearance of peaks at 1644 cm^{-1} related to the C-N and C = O bonds, which was also noted by other researchers investigating isocyanate modification of cellulose fillers (Celebi et al. 2022). In the 1000–1500 cm^{-1} range, multiple weaker signals related to the vibrations of C-C, C-O, C-H, C-N, and N-H bonds. They included bands around 1270 cm^{-1}, characteristic of PBAT (Mohanty and Nayak 2012), and around 1020 cm^{-1}, typical for cellulose (Salmén and Bergström 2009). Moreover, the signal at 726 cm^{-1}, usually observed for a hydrocarbon chain consisting of four or more consecutive methylene groups, was noted for all samples due to the application of PBAT as a matrix (Elfehri Borchani et al. 2015). Generally, presented FTIR spectra revealed the presence of chemical interactions between isocyanates applied as cellulose modifiers and functional groups present on the surface of filler particles or functional groups present in the structure of polymers applied as a matrix for prepared composites (Borrero-López et al. 2021b).

Figure 5 presents the samples' contact angle values to visualize the changes in surface polarity associated with the cellulose filler modifications. The initial value of the contact angle for the Mater-Bi/PCL blend was 88.5 °, which is in line with the literature data presented for Mater-Bi (Aldas et al. 2020b, 2021), PBAT (Fu et al. 2020), and PCL (Mohd Sabee et al. 2022). Therefore, it can be considered a rather hydrophobic material (Law 2014). The incorporation of cellulose filler slightly reduced the contact angle to 86.8° due to the cellulose's polar and hydrophilic nature (Andresen et al. 2006). A similar effect was noted by Tsou et al. (Tsou et al. 2022), who introduced distiller's grains into a poly(ethylene terephthalate) matrix, which for 25% filler loading, reduced the contact angle from 91.3° to 87.0°. However, modification of applied cellulose filler with diisocyanates noticeably increased contact angle to 93.5°, 97.7°, and 92.4°, respectively, for HDI, MDI, and TDI, which was attributed to the reduced polarity of

modified fillers reported in previous work (Hejna et al. 2021c). Ly et al. (Ly et al. 2008) confirmed that reporting a gradual increase of cellulose and lignin pulp contact angles from 47° and 65° to 86° and 90°, respectively, after diisocyanate modifications with 1,4-phenylene diisocyanate and MDI. As a result, prepared materials containing isocyanate-modified fillers could be considered more hydrophobic than the Mater-Bi/PCL blend, which may slightly affect the potential biodegradability of analyzed materials.

Figure 6 and Table 1 summarize the results obtained during the thermogravimetric analysis of prepared materials. The thermal stability of the polymer blend applied as the matrix for analyzed composites is in line with the literature data regarding the stability of its particular components. Elfehri Borchani et al. (Elfehri Borchani et al. 2015) investigated the thermal degradation of Mater-Bi grade NF803 and its composites. They reported the value of temperature at 5 wt.% mass loss ($T_{-5\%}$) of 281.9°C. The value of 286°C was reported in another work by Aldas et al. (Aldas et al. 2020a) for NF866 grade characterized by a relatively similar composition. Comparable values were reported by Nayak et al. (Nayak 2010) for PBAT/TPS blends with varying TPS shares. In the presented study, a higher value of 306.3°C was noted, which was attributed to the 30 wt.% share of PCL in the blend, which is characterized by higher thermal stability, as reported by other authors (Mofokeng and Luyt 2015) or in our previous work (Hejna et al. 2020b). Table 1 also presents the values of thermal decomposition onset attributed to the 2 wt.% mass loss ($T_{-2\%}$), which were in the range of 195–211°C. Such values are attributed to the high content of thermoplastic starch in prepared materials, which shows noticeably lower thermal stability than PBAT or PCL (Mahmood et al. 2017). Considering the course of decomposition, the polymer blend applied as a matrix is characterized by two-step decomposition. The differential thermogravimetric (DTG) curve presented in Fig. 6 shows two prominent peaks at 324.7 and 418.2°C. The first is characteristic of thermoplastic starch degradation, while the second is for polybutylene adipate terephthalate and poly(ε-caprolactone) (Nayak 2010; Mofokeng and Luyt 2015). Moreover, a minor peak at 368.2°C was noted, which was attributed to the degradation of compatibilizing agents present in Mater-Bi (Aldas et al. 2020a).

The introduction of cellulose filler deteriorated the thermal stability of the unfilled polymer blend, which is typical for applying lignocellulosic fillers (Hejna et al. 2021b). However, the first peak on the DTG curve can hardly be noted in composites' curves and is present only as a small shoulder peak near T_{max2} one. Such an effect is attributed to the characteristics of applied UFC100 cellulose filler, whose maximum degradation temperature is around 338°C (Hejna et al. 2021d). Therefore, in the case of composite samples, the cellulose signal overlaps with the T_{max1} peak characteristic for thermoplastic starch and a minor peak associated with modifiers' decomposition, resulting in a T_{max2} shift towards lower temperature. It should be emphasized that the temperature range of the onset of degradation exceeds the melt processing temperature used and recommended for the analyzed materials.

Interestingly, the modification of fillers with different isocyanates enhanced composites' stability, which two phenomena can explain. First is improved compatibility of analyzed systems and enhanced interfacial interactions, which was reported for poly(ε-caprolactone) filled with isocyanate-modified

UFC100 filler in our previous work (Hejna and Kosmela 2020). Such an effect beneficially affects composites' thermal stability, as reported by Kim et al. (Kim et al. 2006). The second phenomenon is the higher thermal stability of fillers themselves resulting from isocyanate modification indicated in other work (Hejna et al. 2021d). Therefore, a noticeable shift of T_{max2} towards higher temperatures was noted.

Table 1
The results of thermogravimetric analysis performed for prepared samples

Sample	$T_{-2\%}$, °C	$T_{-5\%}$, °C	$T_{-10\%}$, °C	$T_{-50\%}$, °C	T_{max1}, °C	T_{max2}, °C	T_{max3}, °C	Residue, wt.%
Blend	210.6	306.3	323.8	411.3	324.7	368.2	418.2	2.38
UFC100	195.1	303.5	328.2	402.5	-	355.0	420.7	3.16
HDI	203.3	301.1	329.2	400.4	-	374.1	421.5	5.83
MDI	205.6	306.1	335.7	400.9	-	370.5	419.9	6.71
TDI	200.3	296.8	332.2	398.8	-	369.3	422.4	5.38

The introduction of modified fillers significantly increased the residue content, which could indicate that char formed during the decomposition of urethane bonds resulting from reactions between isocyanates and hydroxyl groups of cellulose might act as a decomposition inhibitor. Such an effect would be in line with the charring behavior of polyurethanes (Hejna 2021)

Figure 7 and Table 2 present the results of the DSC analysis performed for considered materials. Due to the multi-component composition of Mater-Bi, multiple signals were observed in obtained thermograms. On the cooling curves, two distinct peaks were noted in the range of 10–35°C (peak values from 18.7 to 29.3°C) and 80–115°C (peak values from 91.2 to 111.3°C), which were associated with the crystallization of PCL and PBAT phases of blend and composites (Pagno et al. 2020). The crystallization temperature (T_c) of PCL and PBAT phases was slightly increased after the introduction of as-received and HDI-modified UFC100 filler, indicating that the presence of these fillers facilitates the formation of the crystalline phase. For MDI and TDI modifications, such effects were not noted because of the noticeably higher hydrophobicity resulting from applied treatments or the enhanced interfacial interactions in the isocyanate-modified composites, which may limit the movements of the macromolecules (Hejna et al. 2021c).

Three separate signals were noted on the heating curves, which aligns with the literature data on Mater-Bi polymeric blends (Aldas et al. 2020a). Typically peak attributed to the melting of the PCL phase is hardly noticed in neat Mater-Bi, due to its relatively low content (estimated as below 10%) (Aldas et al. 2020a). However, in the presented case, the blending of Mater-Bi with PCL in a 70:30 ratio resulted in a very noticeable signal on the heating thermogram. The PCL phase's melting temperature (T_m) was at a relatively similar level for unfilled blend and composites containing isocyanate-modified fillers. At the

same time, a noticeable increase from 56.1–56.6°C to 59.2°C was observed for UFC100 as-received cellulose filler. Such an effect may point to the generation of a more perfect crystalline structure ascribed to the introduction of solid particles (Ning et al. 2012). The application of isocyanate treatment hindered these effects, and the melting temperature is similar to the case of the unfilled blend. In the case of the MDI, HDI, and TDI samples, the reduced ΔH_m values for the PCL phase were also reported, which point to the reduction of its crystallinity after the incorporation of modified fillers. This phenomenon may also be connected with the partial reactivity of isocyanates with polymers contained in a blend. In effect, for the isocyanate-modified series, the creation not only of a physical network of the filler in polymeric bulk, as for the UFC100 series, but also a partially crosslinked structure in the interfacial region reduced the mobility of the macromolecules was achieved.

Moreover, two meager peaks were noted around 127–136°C and 147–151°C, which were attributed to the melting of PBAT and thermoplastic starch, respectively (Elfehri Borchani et al. 2015). The most significant shifts in PBAT T_m temperatures are in line with increased melting enthalpy and suggest the improved ability to form crystalline phases of PCL/PBAT-based composites in comparison to the reference blend, which may point to the nucleation ability of cellulose particles, as suggested by other works (Kale et al. 2018; Botta et al. 2021). A similar effect was noted in our previous work on Mater-Bi-based composites filled with brewers' spent grain (Hejna et al. 2022). The peaks attributed to the PCL were significantly bigger, indicating noticeably higher crystallinity than the PBAT phase. However, the presented results cannot give a full description of the exact physical phenomena behind the reported changes in the crystallization and melting of the polymeric blend due to the addition of the as-received and modified cellulose.

Table 2
The results of DSC analysis performed for prepared samples

Sample	T_{mPCL}, °C	ΔH_{mPCL}, J/g	T_{mPBAT}, °C	$T_{mStarch}$, °C	T_{cPCL}, °C	T_{cPBAT}, °C
Blend	56.6	-23.51	129.5	147.2	27.2	101.7
UFC100	59.2	-16.31	135.2	150.9	28.5	106.0
HDI	56.5	-14.54	133.8	149.2	29.3	111.3
MDI	56.5	-14.92	133.9	149.5	25.5	104.9
TDI	56.1	-13.73	127.2	150.2	18.7	91.2

'o indirectly assess the compatibility and interactions between the components of the blend and the omposites produced on their basis and the impact of modification of the composition with the use of arious isocyanates, oscillatory rheological measurements were carried out. Figure 8 presents the results, ncluding complex viscosity (η*), storage (G'), and loss (G") modulus as a function of angular frequency ω) curves, as well as Cole-Cole and van Gurp-Palmen (VGP) plots charts, allowing for the assessment of ompatibility and miscibility of polymer systems in the molten state. All the analyzed materials showed a

course of the complex viscosity curve without the first Newtonian region at low angular frequencies. This effect was described in the literature (Shin et al. 2004) and resulted from a significant amount of filler (starch and cellulose) in the polymer bulk. Rigid domains of the filler became steric hindrances, significantly limiting the mobility of the molten polymer chains and occurring filler-filler interactions (Huang and Zhang 2009). For all composite series, the values of the composites' viscosity are higher than for the blend used as the composite matrix. In the entire angular frequency range, the as-received UFC100 caused the most significant viscosity increase, at least one order of magnitude higher than non-filled with cellulosic filler blends. The addition of isocyanates caused a decrease in viscosity compared to the UFC100 series. This effect is probably related to the surface modification of the fillers, resulting from the reaction of isocyanate groups with hydroxyl groups on the cellulose filler's surface (Nuryawan and Alamsyah 2018). MDI-modified samples showed the most favorable rheological properties. Curves showing changes in G' and G" as the ω function allow describing the characteristic rheological behavior during the measurement. For non-filled blends and MDI-modified composites, a dominant share of viscous properties can be noted in the higher angular frequency values range. In contrast, the material series containing UFC100 is characterized by a predominant share of elastic properties in the whole ω range, which takes from the physical interaction and mutual contact of the fillers in the molten polymer (Barczewski and Mysiukiewicz 2018a)

Comparison of rheological oscillatory data results in the form of Cole-Cole plots, i.e., changes of η" in the η' function, allow for a qualitative assessment of the miscibility or compatibility of the polymeric blends and composites. It is assumed that the material can be described as compatible or miscible when the curves are arranged as smooth semicircle shapes. With the increasing deviation from the model curve, which considers the flattening of the curves in the range of high viscosity values, the results indicate the occurrence of chemical interactions (in the case of partially crosslinked polymers) or the presence of physical interactions in the polymer bulk. In the second case, it can be caused by the lack of miscibility of two polymers limiting the possibility of deformation of the main chains or long chain branches or physical limitation of the mobility of macromolecules caused by the presence of fillers (Utracki 1988; Wu et al. 2008; Mohammadi et al. 2012; Wang et al. 2017; Coombs et al. 2020). The introduction of 30 wt.% of PCL to Mater-Bi, which is a composite containing starch in its composition (Alvarez et al. 2004), did not change the character of the curve course, and its shape indicates limited miscibility of the system (Aid et al. 2017). From the obtained data, it can be observed that the addition of as-received filler (UFC100) increased the viscosity value in the considered angular frequency range and increased the angle of inclination of the curve. Based on the Cole-Cole curves, it can be concluded that the addition of MDI and TDI positively affected the miscibility of the blend with the filler.

None of the analyzed materials showed the VGP curve characteristic of linear thermoplastic polymers with a dominant share of viscous properties, usually observed when phase angle (δ) is reached at a value close to 90° and no interdependence of changes at low complex modulus (|G*|) (Trinkle and Friedrich 2001; Cailloux et al. 2013; Barczewski and Mysiukiewicz 2018b). Chen and Guo (Chen et al. 2009), analyzing the VGP curves for carbon black-polypropylene composites with the addition of ethylene-acrylic acid copolymer, described a sharp decrease in the range of lower complex modulus as a bump. The

appearance of this phenomenon should be analyzed according to the proposed interpretation as the threshold of rheological percolation due to the formation of filler particle networks or/and a co-continuous phase, which spans the whole composite. This effect is visible only for the curves obtained for UFC100 and HDI composites. Thus, for those containing the filler with the most significant tendency to agglomerate and the filler modified with isocyanate with the lowest effectiveness of impact on the natural filler. Moreover, for the MDI-modified composite series, all points are in the range of the highest δ_{max} values. At the same time, based on the interpretation of VGP curves proposed by Chimeni et al. (Chimeni et al. 2016), higher |G*| values at K_{max} can be interpreted as more compatible systems with better wettability of the filler by polymer, which in this case refers to modified MDI and TDI composite series.

Figure 9 presents the images of brittle fracture surfaces of prepared samples obtained using SEM microscopy made with two magnifications. An unfilled Mater-Bi/PCL blend is characterized by a relatively rough surface with smooth plate-shaped gaps and dispersed spherical particles. Such an appearance is typical for TPS-based blends, e.g., Mater-Bi materials (Elfehri Borchani et al. 2015; Merino et al. 2018; Ibáñez-García et al. 2021). Spherical particles, observed as separate phases, are non-plasticized starch granules, which were also observed by other researchers (Aldas et al. 2020b). Smooth gaps in the continuous phase correspond to the PBAT and PCL phases of the prepared blend, while the rougher part is amorphous TPS.

Incorporating 30 wt.% of cellulose particles into the analyzed blend significantly changed the fracture surface appearance. Roughness was noticeably increased due to the presence of filler particles. Image taken at higher magnification indicates a relatively smooth surface of as-received cellulose particles, as well as filler agglomerates, which points to the insufficient interfacial adhesion between matrix and filler. However, singular pull-outs can be observed. Modifying UFC100 particles with diisocyanates noticeably limited the particles' surface area, related to the chemical interactions between isocyanate groups and cellulose hydroxyls and the deposition of isocyanate on the surface (Hejna et al. 2021d). As an effect the number of filler pull-outs was noticeably reduced, and the interface quality was enhanced, which was expressed by the limited number of voids between the polymer matrix and filler particles. These effects were particularly pronounced for MDI and TDI samples, indicating their higher compatibility than UFC100 and HDI materials.

Figure 10 presents the images obtained using atomic force microscopy, while Table 3 provides data from the images' analysis, which confirms the observations made based on SEM images. However, due to the resolution of AFM, the focus was shifted to the observation of the interface between polymer matrix and cellulose filler. Compared to the composites, the unfilled blend's cross-sectional area is noticeably smoother and more homogenous, which was expressed by the lower magnitude of the phase shift angle, and the R_q and R_a values were noticeably lower than for prepared composites. Images also indicated the presence of non-plasticized granules of starch homogenously distributed in the material, confirming results reported in other work (Aldas et al. 2020b).

Observation of UFC100 composite containing as-received cellulose filler revealed poor interface quality, which can be seen in AFM images. Due to the low interfacial adhesion, filler particles were ripped out of the sample surface during preparation. Images indicate that the interfacial area was relatively smooth, which was in line with the conclusions drawn from the analysis of SEM images. Observations have been confirmed by the quantitative analysis of AFM images. The interfacial area of the UFC sample was characterized by a noticeably lower surface area than diisocyanate-modified composites. Modifying filler particles with diisocyanates noticeably enhanced the interfacial adhesion and changed the interface's structure. Presented images show reduced roughness of the cross-sectional area, especially for the TDI sample, which points to the increased compatibility between phases. Moreover, the presence of rough structures at the interface was revealed, which was attributed to the deposition of diisocyanates on the surface of filler particles, as presented in our previous work on diisocyanate modification of cellulose fillers (Hejna et al. 2021d). It was confirmed by the increased R_q and R_a parameters of the interfacial area. Moreover, the negative R_{sk} values point to the layered character of the interface, which confirms the efficient modification of cellulose fillers with diisocyanate and the complete modification of their surface rather than the presence of only spot deposits of the modifier (Duboust et al. 2017). As a result of applied treatments and resulting increased hydrophobicity of fillers, interfacial adhesion to the Mater-Bi/PCL matrix was enhanced.

Table 3
The parameters describing roughness of cross-sectional areas of studied samples, determined by AFM analysis.

Sample	Whole image				1 mm^2 square covering the interface				
	Image size, μm^2	Surface area, 10^3 μm^2	R_q, °	R_a, °	Surface area, μm^2	R_q, °	R_a, °	R_{sk}	R_{ku}
Blend	225	54.1	5.7	4.2	-	-	-	-	-
	25	10.1	5.2	3.5	-	-	-	-	-
UFC	225	47.6	13.6	9.6	231	13.9	11.6	0.32	2.25
	25	17.3	10.9	8.0	501	9.7	6.9	0.36	5.55
HDI	225	98.3	17.5	13.3	382	15.9	12.6	-0.81	3.18
	25	16.9	12.9	9.6	779	14.0	11.2	-0.71	3.50
MDI	225	83.5	13.8	10.2	385	11.7	8.9	-0.88	4.14
	25	19.6	14.2	9.9	1178	20.9	16.1	-0.79	6.03
TDI	225	69.5	12.0	9.1	320	11.7	8.2	-1.95	8.29
	25	13.6	9.64	7.1	653	10.3	8.0	-0.47	12.03

4. Conclusions

Both surface and bulk properties of biocomposites are changed by incorporation of cellulose fillers as well as its surface modification with HDI, MDI, or TDI. Analysis of FTIR spectra exhibited the presence of chemical interlocking between isocyanates applied as cellulose modifiers and functional groups present on the surface of cellulose particles or those present in the structure of Mater-Bi and PCL reference blends. The newly formed chemical interactions resulted in an increased hydrophobicity, which can be attributed to the partial attraction between polar functional groups of isocyanate and amine functionalities of fillers. Contact angle measurements supported such chemically modified interactions, by obvious increase in contact angle from 88.5 ° for Mater-Bi/PCL blend to 93.5°, 97.7°, and 92.4° for biocomposites possessing HDI-, MDI-, and TDI-modified cellulose filler, respectively. This was additionally confirmed by the rougher fracture surface and cross-sectional areas observed for biocomposites by the SEM and AFM, where an enhanced interfacial adhesion was likely. Due to the improved compatibility of composites containing modified fillers, as suggested by the rheological analysis and Cole-Cole and VGP plots, their thermal stability was slightly enhanced, which was expressed by a shift in the temperature attributed to the onset of thermal decomposition towards higher temperatures. The presence of diisocyanate-modified cellulose increased the amount residue remained from TGA testing, resulting from the reaction between isocyanates and hydroxyl groups of cellulose possibly acting act as a decomposition inhibitor. Addition of as-received cellulose to Mater-Bi/PCL sustainable blends increased the viscosity in the studied angular frequency range, particularly the angle of inclination of the curve. Based on the Cole-Cole and VGP plots, addition of MDI and TDI positively affected the miscibility of the blend. However, the incorporation of diisocyanate-modified fillers did not saliently affect the crystallinity of polymer matrix. Therefore, it can be anticipated that due to the enhancement of interface, the mechanical performance of composites would benefit from filler treatment, while the rate of their potential biodegradation would not be affected.

Declarations

Ethics approval and consent to participate

Not applicable

Consent for publication

Not applicable

Availability of data and materials

Data available on request

Competing interests

The authors declare that they have no known competing financial interests or personal relationships that could have appeared to influence the work reported in this paper.

Funding

This work was supported by the National Science Centre (NCN, Poland) in the frame of SONATINA 2 project 2018/28/C/ST8/00187 - Structure and properties of lignocellulosic fillers modified in situ during reactive extrusion. The study was partially co-funded under project with grants for education allocated by the Ministry of Science and Higher Education in Poland executed under the subject of No 0613/SBAD/4820.

Authors' contributions

Conceptualization: A.H.; Data Curation: A.H., M.B., P.K., O.M., A.T., and A.P.; Formal analysis: A.H., M.B., and M.R.S.; Funding acquisition: A.H., M.B., and M.S.; Investigation: A.H., M.B., P.K., O.M., A.T., and A.P.; Methodology: M.B., P.K., O.M., A.T., and A.P.; Project administration: A.H., M.B., and M.S.; Resources: A.H. and M.B.; Software: M.B., P.K., O.M., A.T., and A.P.; Supervision: A.H. and M.B.; Validation: A.H., M.B., A.T., and M.R.S.; Visualization: A.H., M.B., and A.P.; Writing - original draft: A.H., M.B., O.M., and M.R.S.; Writing - review & editing: A.H., M.B., O.M., A.T., and M.R.S.

Acknowledgements

Not applicable

References

1. Abdul Khalil HPS, Tye YY, Saurabh CK, et al (2017) Biodegradable polymer films from seaweed polysaccharides: A review on cellulose as a reinforcement material. Express Polym Lett 11:244–265. https://doi.org/10.3144/expresspolymlett.2017.26
2. Aid S, Eddhahak A, Ortega Z, et al (2017) Experimental study of the miscibility of ABS/PC polymer blends and investigation of the processing effect. J Appl Polym Sci 134:. https://doi.org/10.1002/app.44975
3. Aldas M, Ferri JM, Lopez-Martinez J, et al (2020a) Effect of pine resin derivatives on the structural, thermal, and mechanical properties of Mater-Bi type bioplastic. J Appl Polym Sci 137:48236. https://doi.org/10.1002/app.48236
4. Aldas M, Pavon C, Ferri JM, et al (2021) Films Based on Mater-Bi® Compatibilized with Pine Resin Derivatives: Optical, Barrier, and Disintegration Properties. Polymers (Basel) 13:1506. https://doi.org/10.3390/polym13091506
5. Aldas M, Rayón E, López-Martínez J, Arrieta MP (2020b) A Deeper Microscopic Study of the Interaction between Gum Rosin Derivatives and a Mater-Bi Type Bioplastic. Polymers (Basel) 12:226. https://doi.org/10.3390/polym12010226
6. Alvarez VA, Terenzi A, Kenny JM, Vázquez A (2004) Melt rheological behavior of starch-based matrix composites reinforced with short sisal fibers. Polym Eng Sci 44:1907–1914. https://doi.org/10.1002/pen.20193

7. Andresen M, Johansson L-S, Tanem BS, Stenius P (2006) Properties and characterization of hydrophobized microfibrillated cellulose. Cellulose 13:665–677. https://doi.org/10.1007/s10570-006-9072-1
8. Barczewski M, Mysiukiewicz O (2018a) Rheological and Processing Properties of Poly(lactic acid) Composites Filled with Ground Chestnut Shell. Polymer Korea 42:267–274. https://doi.org/10.7317/pk.2018.42.2.267
9. Barczewski M, Mysiukiewicz O (2018b) Rheological and Processing Properties of Poly(lactic acid) Composites Filled with Ground Chestnut Shell. Polymer Korea 42:267–274. https://doi.org/10.7317/pk.2018.42.2.267
10. Barczewski M, Mysiukiewicz O, Hejna A, et al (2021) The Effect of Surface Treatment with Isocyanate and Aromatic Carbodiimide of Thermally Expanded Vermiculite Used as a Functional Filler for Polylactide-Based Composites. Polymers (Basel) 13:890. https://doi.org/10.3390/polym13060890
11. Borchani KE, Carrot C, Jaziri M (2019) Rheological behavior of short Alfa fibers reinforced Mater-Bi® biocomposites. Polym Test 77:105895. https://doi.org/10.1016/j.polymertesting.2019.05.011
12. Borrero-López AM, Guzmán DB, González-Delgado JA, et al (2021a) Toward UV-Triggered Curing of Solvent-Free Polyurethane Adhesives Based on Castor Oil. ACS Sustain Chem Eng 9:11032–11040. https://doi.org/10.1021/acssuschemeng.1c02461
13. Borrero-López AM, Guzmán DB, González-Delgado JA, et al (2021b) Toward UV-Triggered Curing of Solvent-Free Polyurethane Adhesives Based on Castor Oil. ACS Sustain Chem Eng 9:11032–11040. https://doi.org/10.1021/acssuschemeng.1c02461
14. Botta L, Titone V, Mistretta MC, et al (2021) PBAT Based Composites Reinforced with Microcrystalline Cellulose Obtained from Softwood Almond Shells. Polymers (Basel) 13:2643. https://doi.org/10.3390/polym13162643
15. Brockhaus S, Petersen M, Kersten W (2016) A crossroads for bioplastics: exploring product developers' challenges to move beyond petroleum-based plastics. J Clean Prod 127:84–95. https://doi.org/10.1016/j.jclepro.2016.04.003
16. Cailloux J, Santana OO, Franco-Urquiza E, et al (2013) Sheets of branched poly(lactic acid) obtained by one step reactive extrusion calendering process: Melt rheology analysis. Express Polym Lett 7:304–318. https://doi.org/10.3144/expresspolymlett.2013.27
17. Celebi H, Ilgar M, Seyhan AT (2022) Evaluation of the effect of isocyanate modification on the thermal and rheological properties of poly(ε-caprolactone)/cellulose composites. Polymer Bulletin 79:4941–4955. https://doi.org/10.1007/s00289-021-03753-3
18. Chen G, Yang B, Guo S (2009) Ethylene-acrylic acid copolymer induced electrical conductivity improvements and dynamic rheological behavior changes of polypropylene/carbon black composites. J Polym Sci B Polym Phys 47:1762–1771. https://doi.org/10.1002/polb.21778
19. Chimeni DY, Toupe JL, Dubois C, Rodrigue D (2016) Effect of surface modification on the interface quality between hemp and linear medium-density polyethylene. J Appl Polym Sci 133:. https://doi.org/10.1002/app.43802

20. Coombs SJ, Kanso MA, Giacomin AJ (2020) Cole–Cole relation for long-chain branching from general rigid bead–rod theory. Physics of Fluids 32:093106. https://doi.org/10.1063/5.0024402
21. DeArmitt C, Breese KevinD (2001) Filled polypropylene: a cost-performance comparison of common fillers. Plastics, Additives and Compounding 3:28–33. https://doi.org/10.1016/S1464-391X(01)80252-X
22. Duboust N, Ghadbeigi H, Pinna C, et al (2017) An optical method for measuring surface roughness of machined carbon fibre-reinforced plastic composites. J Compos Mater 51:289–302. https://doi.org/10.1177/0021998316644849
23. Elfehri Borchani K, Carrot C, Jaziri M (2015) Biocomposites of Alfa fibers dispersed in the Mater-Bi® type bioplastic: Morphology, mechanical and thermal properties. Compos Part A Appl Sci Manuf 78:371–379. https://doi.org/10.1016/j.compositesa.2015.08.023
24. Ferreira DP, Cruz J, Fangueiro R (2019) Surface modification of natural fibers in polymer composites. In: Green Composites for Automotive Applications. Elsevier, pp 3–41
25. França DC, Almeida TG, Abels G, et al (2019) Tailoring PBAT/PLA/Babassu films for suitability of agriculture mulch application. Journal of Natural Fibers 16:933–943. https://doi.org/10.1080/15440478.2018.1441092
26. Fu Y, Wu G, Bian X, et al (2020) Biodegradation Behavior of Poly(Butylene Adipate-Co-Terephthalate) (PBAT), Poly(Lactic Acid) (PLA), and Their Blend in Freshwater with Sediment. Molecules 25:3946. https://doi.org/10.3390/molecules25173946
27. Haina, Gul S, Awais M, et al (2020) Recent Trends in Preparation and Applications of Biodegradable Polymer Composites. J Renew Mater 8:1305–1326. https://doi.org/10.32604/jrm.2020.010037
28. Haque MdM-U, Alvarez V, Paci M, Pracella M (2011) Processing, compatibilization and properties of ternary composites of Mater-Bi with polyolefins and hemp fibres. Compos Part A Appl Sci Manuf 42:2060–2069. https://doi.org/10.1016/j.compositesa.2011.09.015
29. Hejna A (2021) Clays as inhibitors of polyurethane foams' flammability. Materials 14:. https://doi.org/10.3390/ma14174826
30. Hejna A (2020) Poly(ε-Caprolactone)/Brewers' Spent Grain Composites—The Impact of Filler Treatment on the Mechanical Performance. Journal of Composites Science 4:167. https://doi.org/10.3390/jcs4040167
31. Hejna A, Barczewski M, Kosmela P, et al (2021a) Mandarin peel as an auspicious functional filler for polymer composites. Macedonian Journal of Chemistry and Chemical Engineering 40:89–106
32. Hejna A, Barczewski M, Kosmela P, et al (2022) Mater-Bi/Brewers' Spent Grain Biocomposites—Novel Approach to Plant-Based Waste Filler Treatment by Highly Efficient Thermomechanical and Chemical Methods. Materials 15:7099. https://doi.org/10.3390/ma15207099
33. Hejna A, Korol J, Kosmela P, et al (2021b) By-products from food industry as a promising alternative for the conventional fillers for wood–polymer composites. Polymers (Basel) 13:. https://doi.org/10.3390/polym13060893

34. Hejna A, Kosmela P (2020) Insights into compatibilization of poly(ε-caprolactone)-based biocomposites with diisocyanates as modifiers of cellulose fillers. Mindanao Journal of Science and Technology 18:221–241
35. Hejna A, Marć M, Korol J (2021c) Modification of cellulosic filler with diisocyanates – volatile organic compounds emission assessment and stability of chemical structure over time. Nord Pulp Paper Res J 36:353–372. https://doi.org/10.1515/npprj-2020-0104
36. Hejna A, Marć M, Skórczewska K, et al (2021d) Insights into modification of lignocellulosic fillers with isophorone diisocyanate: structure, thermal stability and volatile organic compounds emission assessment. European Journal of Wood and Wood Products 79:75–90. https://doi.org/10.1007/s00107-020-01604-y
37. Hejna A, Przybysz-Romatowska M, Kosmela P, et al (2020a) Recent advances in compatibilization strategies of wood-polymer composites by isocyanates. Wood Sci Technol 54:. https://doi.org/10.1007/s00226-020-01203-3
38. Hejna A, Sulyman M, Przybysz M, et al (2020b) On the Correlation of Lignocellulosic Filler Composition with the Performance Properties of Poly(ε-Caprolactone) Based Biocomposites. Waste Biomass Valorization 11:1467–1479. https://doi.org/10.1007/s12649-018-0485-5
39. Huang H-X, Zhang J-J (2009) Effects of filler-filler and polymer-filler interactions on rheological and mechanical properties of HDPE-wood composites. J Appl Polym Sci 111:2806–2812. https://doi.org/10.1002/app.29336
40. Ibáñez-García A, Martínez-García A, Ferrándiz-Bou S (2021) Recyclability Analysis of Starch Thermoplastic/Almond Shell Biocomposite. Polymers (Basel) 13:1159. https://doi.org/10.3390/polym13071159
41. Kale RD, Gorade VG, Madye N, et al (2018) Preparation and characterization of biocomposite packaging film from poly(lactic acid) and acylated microcrystalline cellulose using rice bran oil. Int J Biol Macromol 118:1090–1102. https://doi.org/10.1016/j.ijbiomac.2018.06.076
42. Kim H-S, Kim S, Kim H-J, Yang H-S (2006) Thermal properties of bio-flour-filled polyolefin composites with different compatibilizing agent type and content. Thermochim Acta 451:181–188. https://doi.org/10.1016/j.tca.2006.09.013
43. Law K-Y (2014) Definitions for Hydrophilicity, Hydrophobicity, and Superhydrophobicity: Getting the Basics Right. J Phys Chem Lett 5:686–688. https://doi.org/10.1021/jz402762h
44. Liu Y, Lv X, Bao J, et al (2019) Characterization of silane treated and untreated natural cellulosic fibre from corn stalk waste as potential reinforcement in polymer composites. Carbohydr Polym 218:179–187. https://doi.org/10.1016/j.carbpol.2019.04.088
45. Ly B, Thielemans W, Dufresne A, et al (2008) Surface functionalization of cellulose fibres and their incorporation in renewable polymeric matrices. Compos Sci Technol 68:3193–3201. https://doi.org/10.1016/j.compscitech.2008.07.018
46. Mahmood H, Moniruzzaman M, Iqbal T, Yusup S (2017) Effect of ionic liquids pretreatment on thermal degradation kinetics of agro-industrial waste reinforced thermoplastic starch composites. J

Mol Liq 247:164–170. https://doi.org/10.1016/j.molliq.2017.09.106

47. Merino D, Gutiérrez TJ, Mansilla AY, et al (2018) Critical Evaluation of Starch-Based Antibacterial Nanocomposites as Agricultural Mulch Films: Study on Their Interactions with Water and Light. ACS Sustain Chem Eng 6:15662–15672. https://doi.org/10.1021/acssuschemeng.8b04162
48. Mofokeng JP, Luyt AS (2015) Morphology and thermal degradation studies of melt-mixed poly(lactic acid) (PLA)/poly(ε-caprolactone) (PCL) biodegradable polymer blend nanocomposites with TiO2 as filler. Polym Test 45:93–100. https://doi.org/10.1016/j.polymertesting.2015.05.007
49. Mohammadi M, Yousefi AA, Ehsani M (2012) Thermorheological analysis of blend of high- and low-density polyethylenes. Journal of Polymer Research 19:9798. https://doi.org/10.1007/s10965-011-9798-9
50. Mohanty S, Nayak SK (2012) Biodegradable Nanocomposites of Poly(butylene adipate-co-terephthalate) (PBAT) and Organically Modified Layered Silicates. J Polym Environ 20:195–207. https://doi.org/10.1007/s10924-011-0408-z
51. Mohd Sabee MMS, Ahmad Tajuddin NNI, Ku Ishak KM, et al (2022) Comparison of physical and mechanical properties of biodegradable polybutylene adipate terephthalate, polycaprolactone, and poly(lactic acid) fabricated via fused deposition modeling and conventional molding. J Appl Polym Sci 139:. https://doi.org/10.1002/app.52973
52. Mohit H, Arul Mozhi Selvan V (2018) A comprehensive review on surface modification, structure interface and bonding mechanism of plant cellulose fiber reinforced polymer based composites. Compos Interfaces 25:629–667. https://doi.org/10.1080/09276440.2018.1444832
53. Motaung TE, Linganiso LZ (2018) Critical review on agrowaste cellulose applications for biopolymers. International Journal of Plastics Technology 22:185–216. https://doi.org/10.1007/s12588-018-9219-6
54. Nayak SK (2010) Biodegradable PBAT/Starch Nanocomposites. Polym Plast Technol Eng 49:1406–1418. https://doi.org/10.1080/03602559.2010.496397
55. Ning N, Fu S, Zhang W, et al (2012) Realizing the enhancement of interfacial interaction in semicrystalline polymer/filler composites via interfacial crystallization. Prog Polym Sci 37:1425–1455. https://doi.org/10.1016/j.progpolymsci.2011.12.005
56. Nuryawan A, Alamsyah EM (2018) A Review of Isocyanate Wood Adhesive: A Case Study in Indonesia. In: Applied Adhesive Bonding in Science and Technology. InTech
57. Pagno V, Módenes AN, Dragunski DC, et al (2020) Heat treatment of polymeric PBAT/PCL membranes containing activated carbon from Brazil nutshell biomass obtained by electrospinning and applied in drug removal. J Environ Chem Eng 8:104159. https://doi.org/10.1016/j.jece.2020.104159
58. Platnieks O, Gaidukovs S, Barkane A, et al (2020) Bio-Based Poly(butylene succinate)/Microcrystalline Cellulose/Nanofibrillated Cellulose-Based Sustainable Polymer Composites: Thermo-Mechanical and Biodegradation Studies. Polymers (Basel) 12:1472. https://doi.org/10.3390/polym12071472

59. RameshKumar S, Shaiju P, O'Connor KE, P RB (2020) Bio-based and biodegradable polymers - State-of-the-art, challenges and emerging trends. Curr Opin Green Sustain Chem 21:75–81. https://doi.org/10.1016/j.cogsc.2019.12.005
60. Ruggero F, Carretti E, Gori R, et al (2020) Monitoring of degradation of starch-based biopolymer film under different composting conditions, using TGA, FTIR and SEM analysis. Chemosphere 246:125770. https://doi.org/10.1016/j.chemosphere.2019.125770
61. Salmén L, Bergström E (2009) Cellulose structural arrangement in relation to spectral changes in tensile loading FTIR. Cellulose 16:975–982. https://doi.org/10.1007/s10570-009-9331-z
62. Shaghaleh H, Xu X, Wang S (2018) Current progress in production of biopolymeric materials based on cellulose, cellulose nanofibers, and cellulose derivatives. RSC Adv 8:825–842. https://doi.org/10.1039/C7RA11157F
63. Shin BY, Lee S Il, Shin YS, et al (2004) Rheological, mechanical and biodegradation studies on blends of thermoplastic starch and polycaprolactone. Polym Eng Sci 44:1429–1438. https://doi.org/10.1002/pen.20139
64. Srebrenkoska V, Bogoeva Gaceva G, Dimeski D (2014) Biocomposites based on polylactic acid and their thermal behavior after recycing. Macedonian Journal of Chemistry and Chemical Engineering 33:277. https://doi.org/10.20450/mjcce.2014.479
65. Szefer E, Leszczyńska A, Pielichowski K (2018) Modification of microcrystalline cellulose filler with succinic anhydride - effect of microwave and conventional heating. Composites Theory and Practice 18:25–31
66. Trinkle S, Friedrich C (2001) Van Gurp-Palmen-plot: a way to characterize polydispersity of linear polymers. Rheol Acta 40:322–328. https://doi.org/10.1007/s003970000137
67. Tsou C-H, Ma Z-L, Yang T, et al (2022) Reinforced distiller's grains as bio-fillers in environment-friendly poly(ethylene terephthalate) composites. Polymer Bulletin. https://doi.org/10.1007/s00289-022-04318-8
68. Utracki LA (1988) Viscoelastic behavior of polymer blends. Polym Eng Sci 28:1401–1404. https://doi.org/10.1002/pen.760282109
69. Wang FC, Feve M, Lam TM, Pascault J-P (1994) FTIR analysis of hydrogen bonding in amorphous linear aromatic polyurethanes. I. Influence of temperature. J Polym Sci B Polym Phys 32:1305–1313. https://doi.org/10.1002/polb.1994.090320801
70. Wang H, Yang X, Fu Z, et al (2017) Rheology of Nanosilica-Compatibilized Immiscible Polymer Blends: Formation of a "Heterogeneous Network" Facilitated by Interfacially Anchored Hybrid Nanosilica. Macromolecules 50:9494–9506. https://doi.org/10.1021/acs.macromol.7b02143
71. Wang L, Hu J, Liu Y, et al (2020) Ionic Liquids Grafted Cellulose Nanocrystals for High-Strength and Toughness PVA Nanocomposite. ACS Appl Mater Interfaces 12:38796–38804. https://doi.org/10.1021/acsami.0c11217
72. Wu D, Zhang Y, Zhang M, Zhou W (2008) Phase behavior and its viscoelastic response of polylactide/poly(ε-caprolactone) blend. Eur Polym J 44:2171–2183.

https://doi.org/10.1016/j.eurpolymj.2008.04.023

73. Wu R (2022) An Empirical Investigation of the Economic Impacts of COVID-19: Micro-level Evidence from Europe. Int Rev Appl Econ 36:675–696. https://doi.org/10.1080/02692171.2022.2040961
74. Xie X, Zhang C, Weng Y, et al (2020) Effect of Diisocyanates as Compatibilizer on the Properties of BF/PBAT Composites by In Situ Reactive Compatibilization, Crosslinking and Chain Extension. Materials 13:806. https://doi.org/10.3390/ma13030806
75. Yang Y, Zhang L, Zhang J, et al (2023) Reengineering Waste Boxwood Powder into Light and High-Strength Biodegradable Composites to Replace Petroleum-Based Synthetic Materials. ACS Appl Mater Interfaces 15:4505–4515. https://doi.org/10.1021/acsami.2c19844
76. Yu S, Wang H-M, Xiong S-J, et al (2022) Sustainable Wood-Based Poly(butylene adipate-*co*-terephthalate) Biodegradable Composite Films Reinforced by a Rapid Homogeneous Esterification Strategy. ACS Sustain Chem Eng 10:14568–14578. https://doi.org/10.1021/acssuschemeng.2c04332

Figures

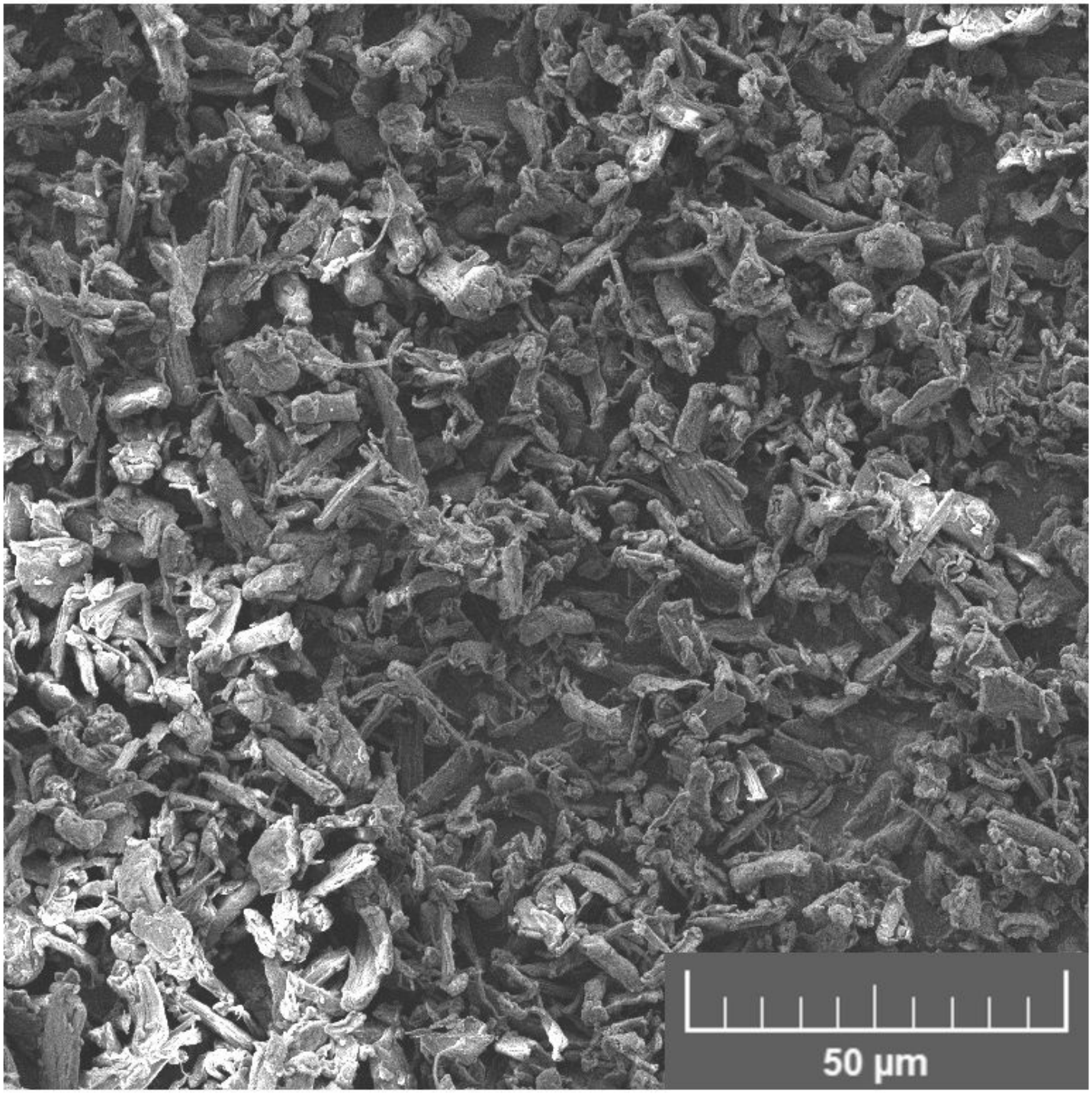

Figure 1

SEM micrograph of as-received UFC100 cellulose filler.

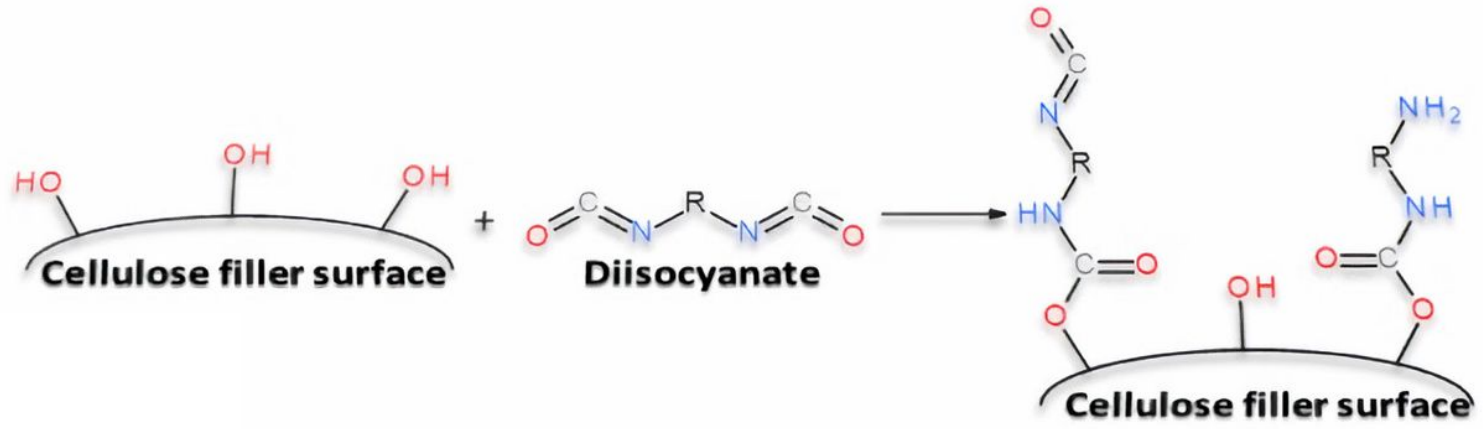

Figure 2

Scheme of the potential interactions between filler particles and applied diisocyanate modifiers.

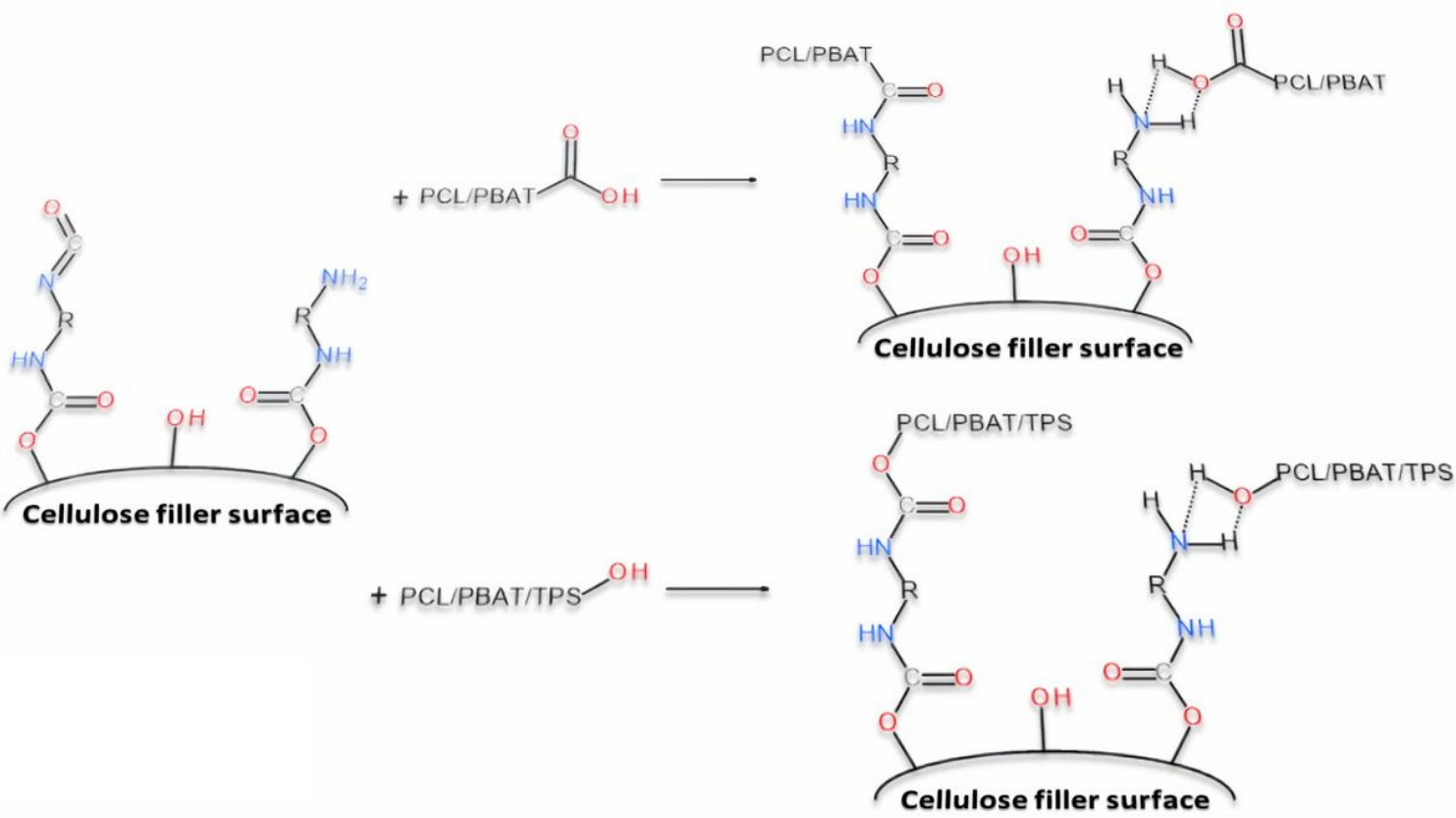

igure 3

cheme of the potential interfacial interactions between modified cellulose fillers and components of the olymer matrix.

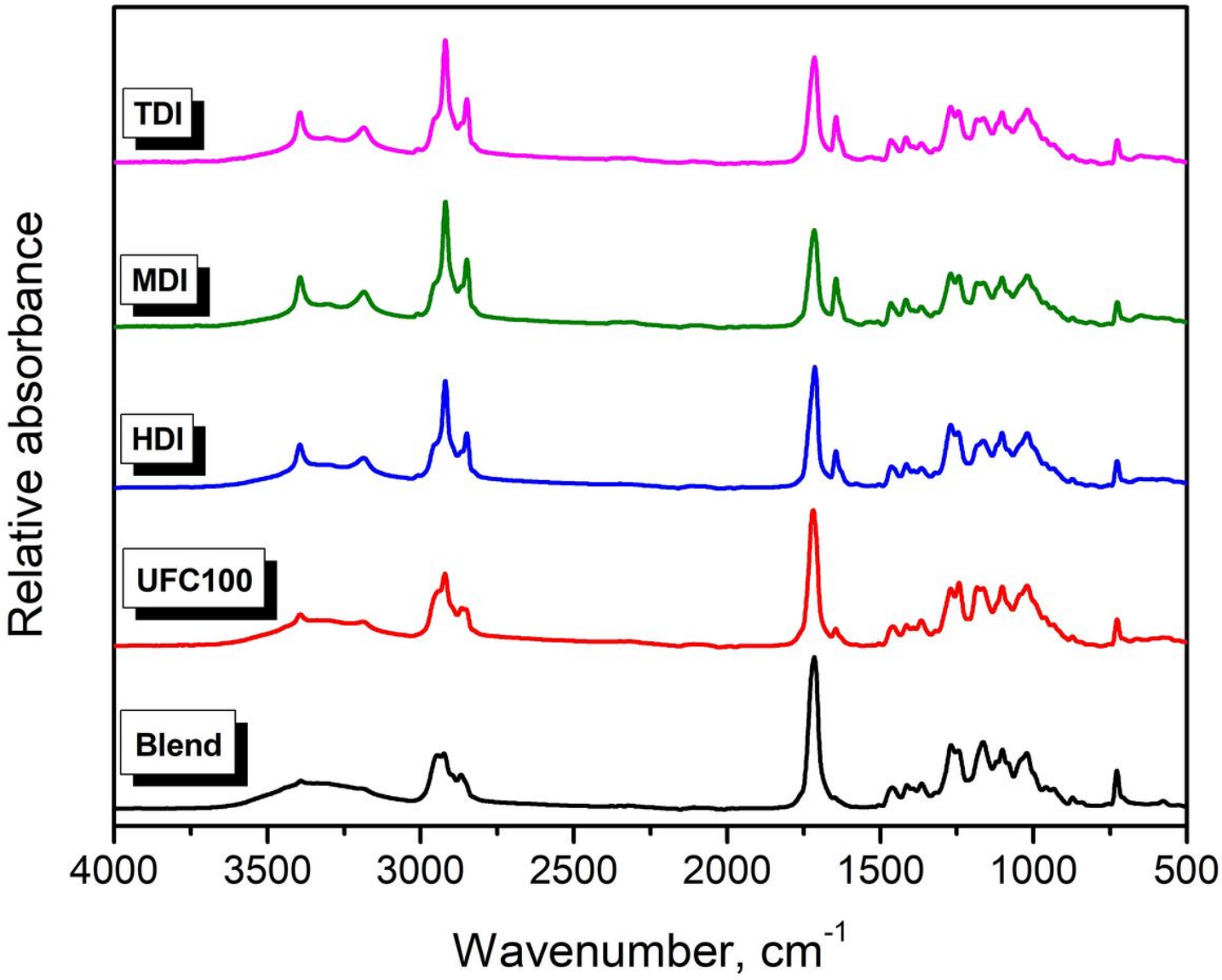

Figure 4

FTIR spectra of unfilled Mater-Bi/PCL blend and composite samples.

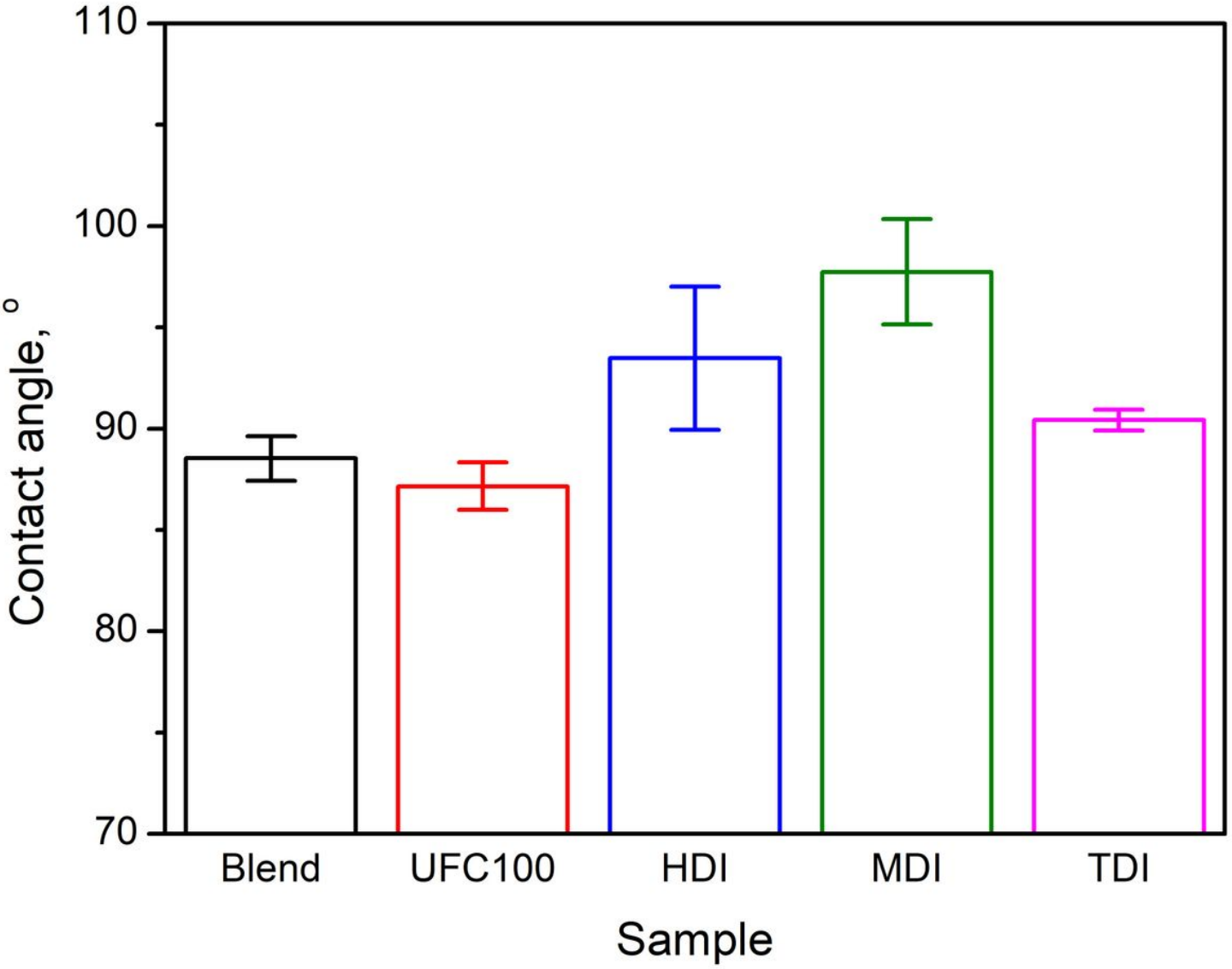

Figure 5

Values of the water contact angle determined for the prepared samples.

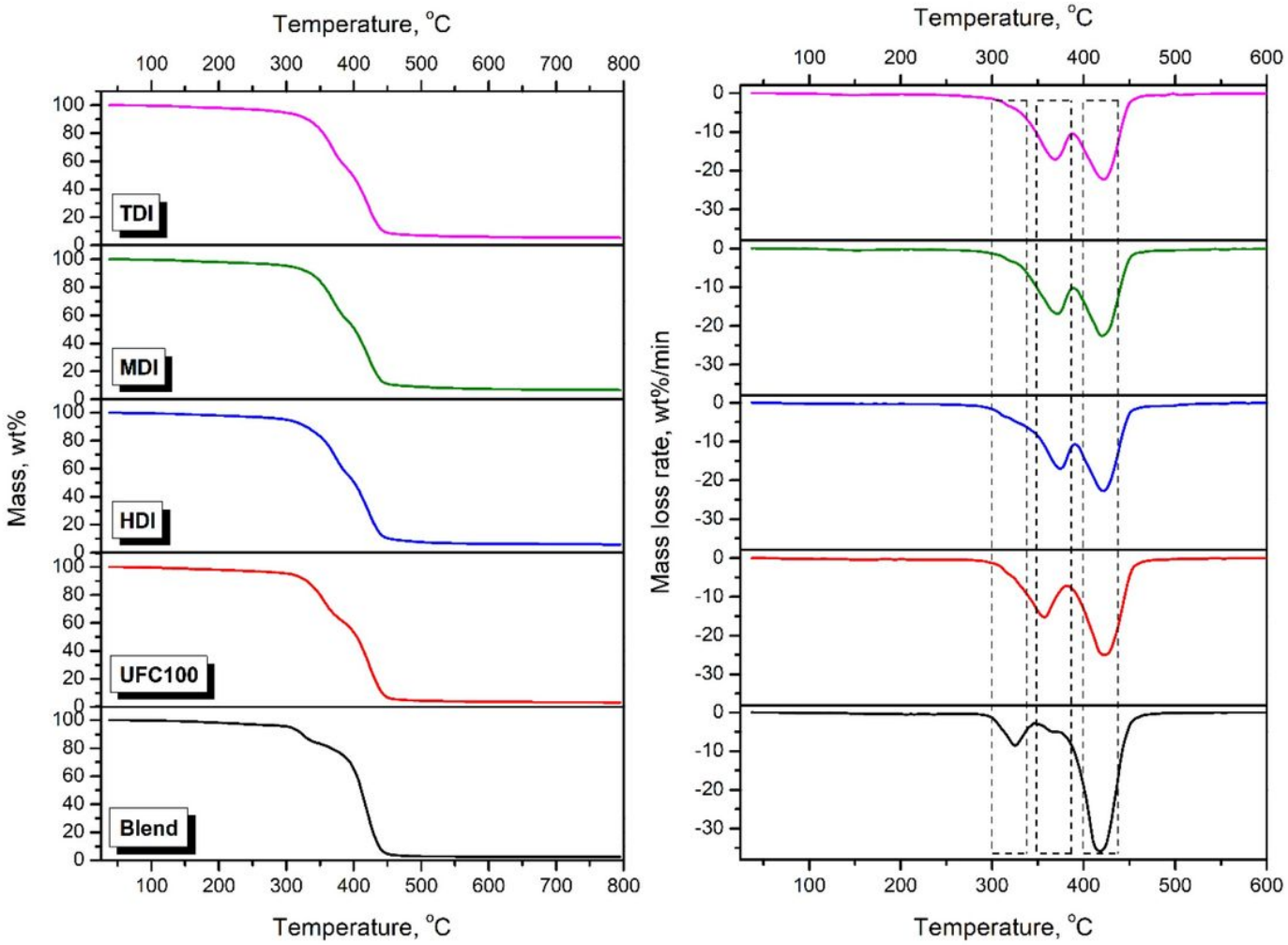

Figure 6

Mass loss curves (left) and differential thermogravimetric curves (right) visualizing the course of prepared samples' thermal decomposition.

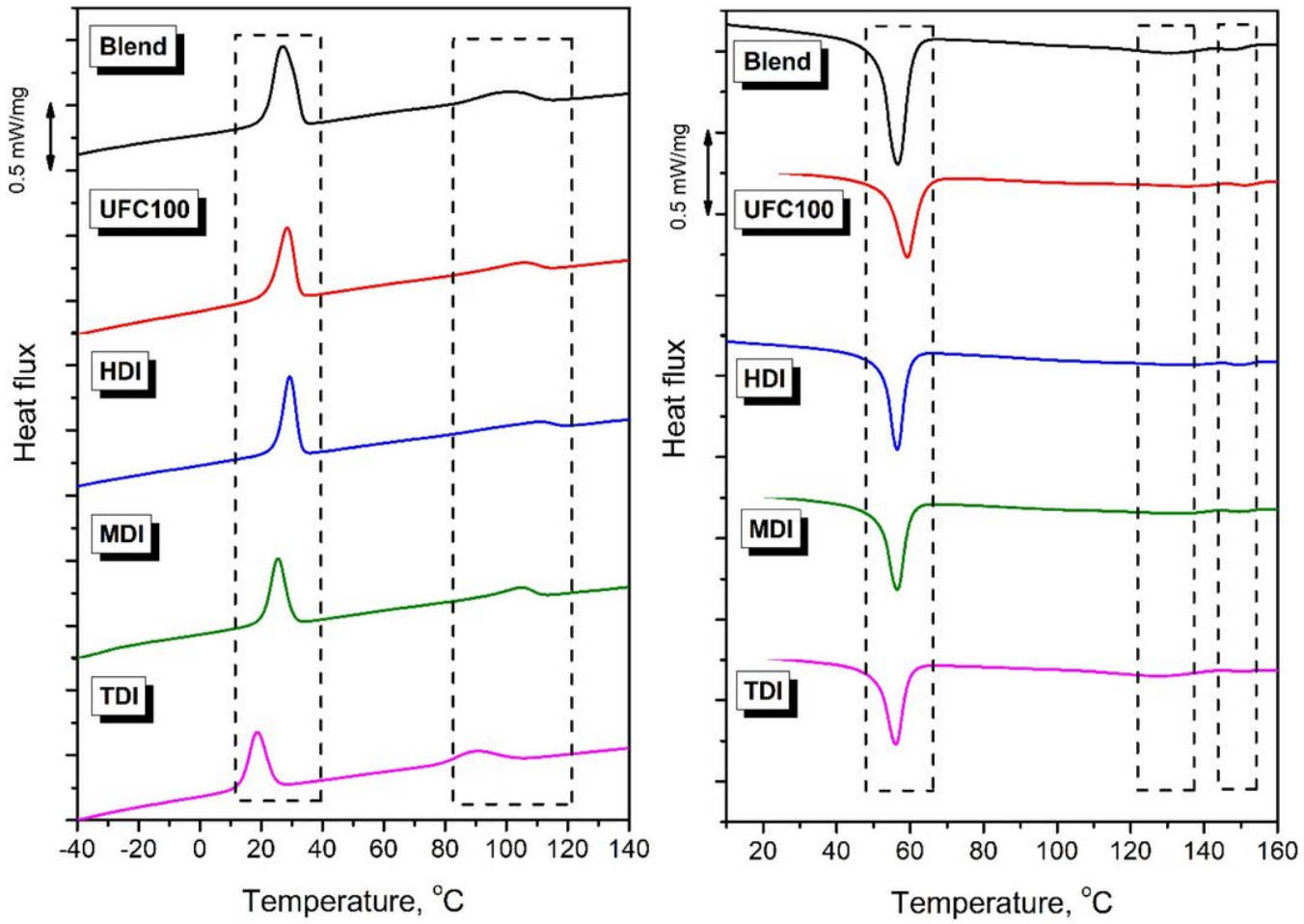

Figure 7

Cooling (left) and heating (right) thermograms obtained during DSC analysis of prepared samples (exo ↑).

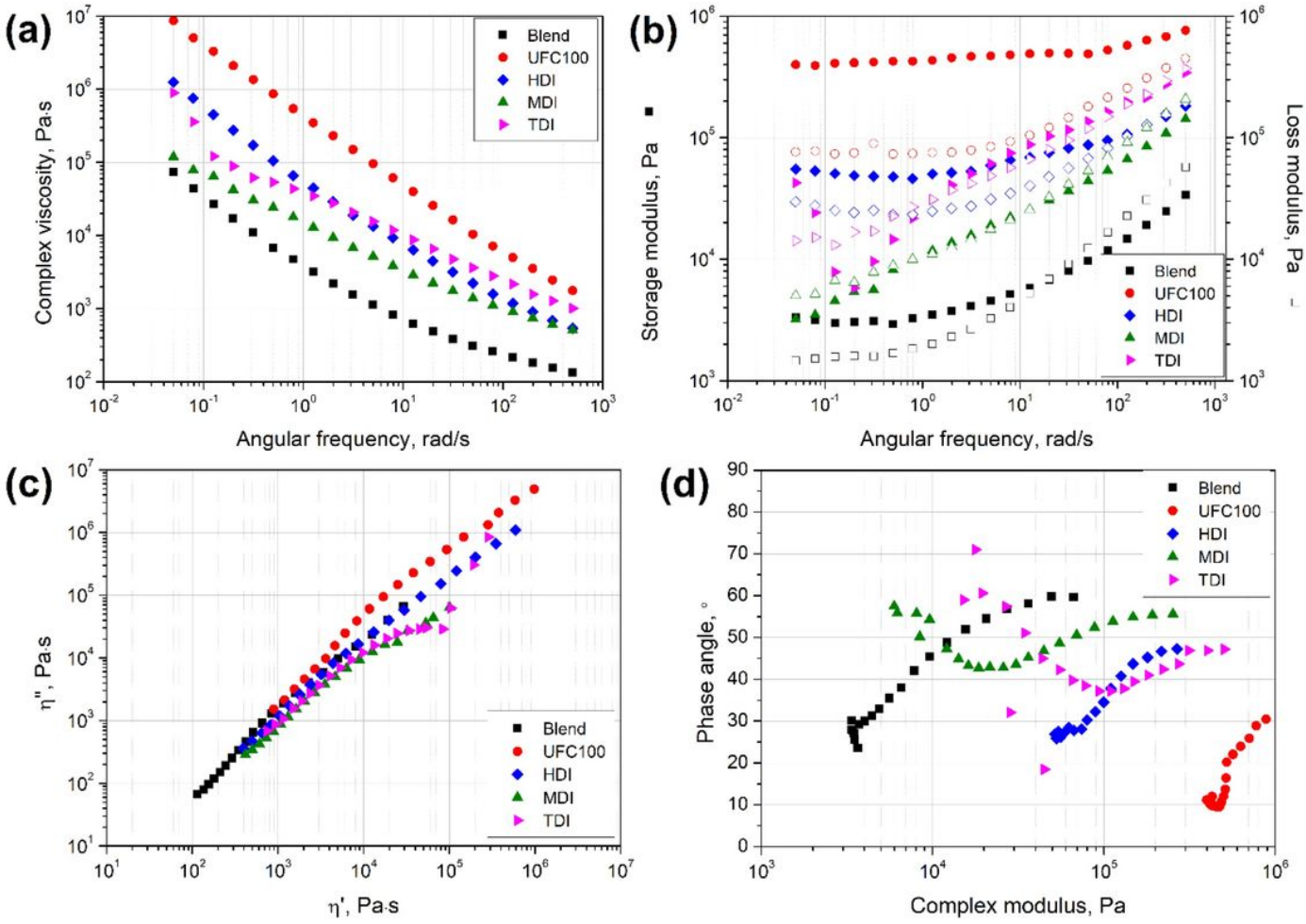

Figure 8

Complex viscosity curves (a), storage and loss modulus as a function of angular frequency (b), Cole-Cole plots (c) and van Gurp-Palmen plots (d) of prepared samples.

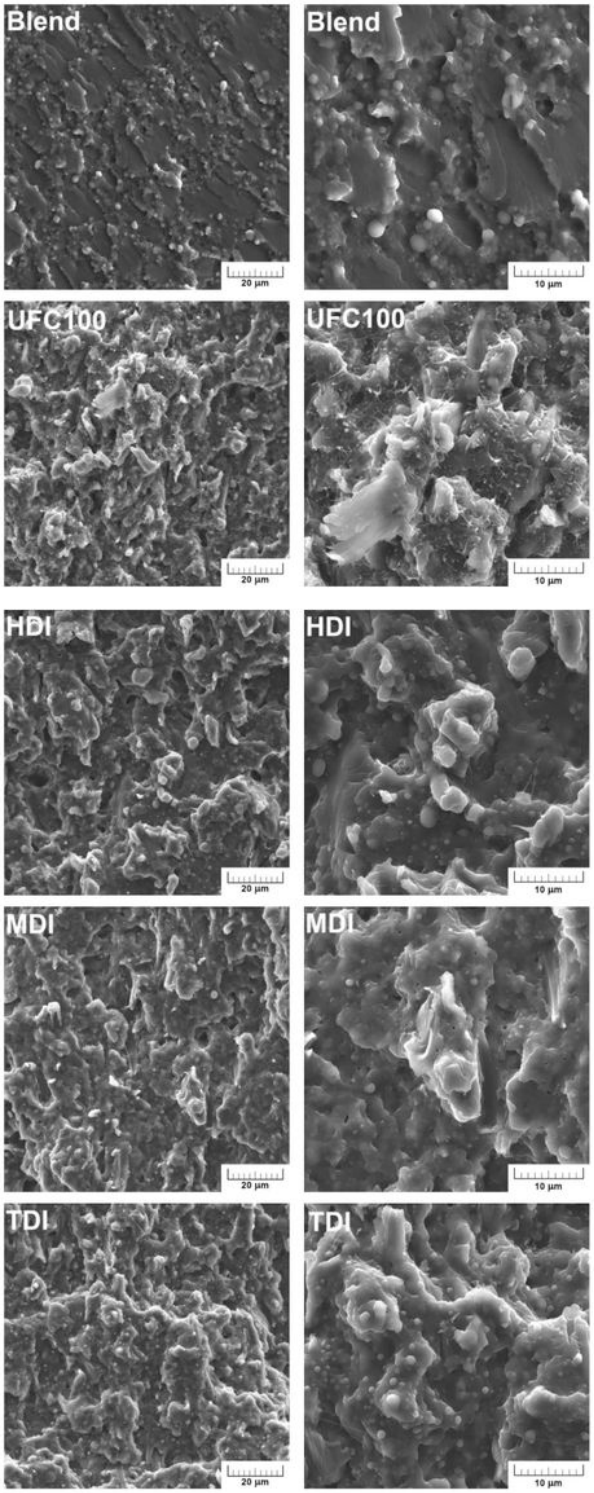

igure 9

EM images of prepared samples' brittle fracture surfaces at different magnifications; lower (left) and igher (right).

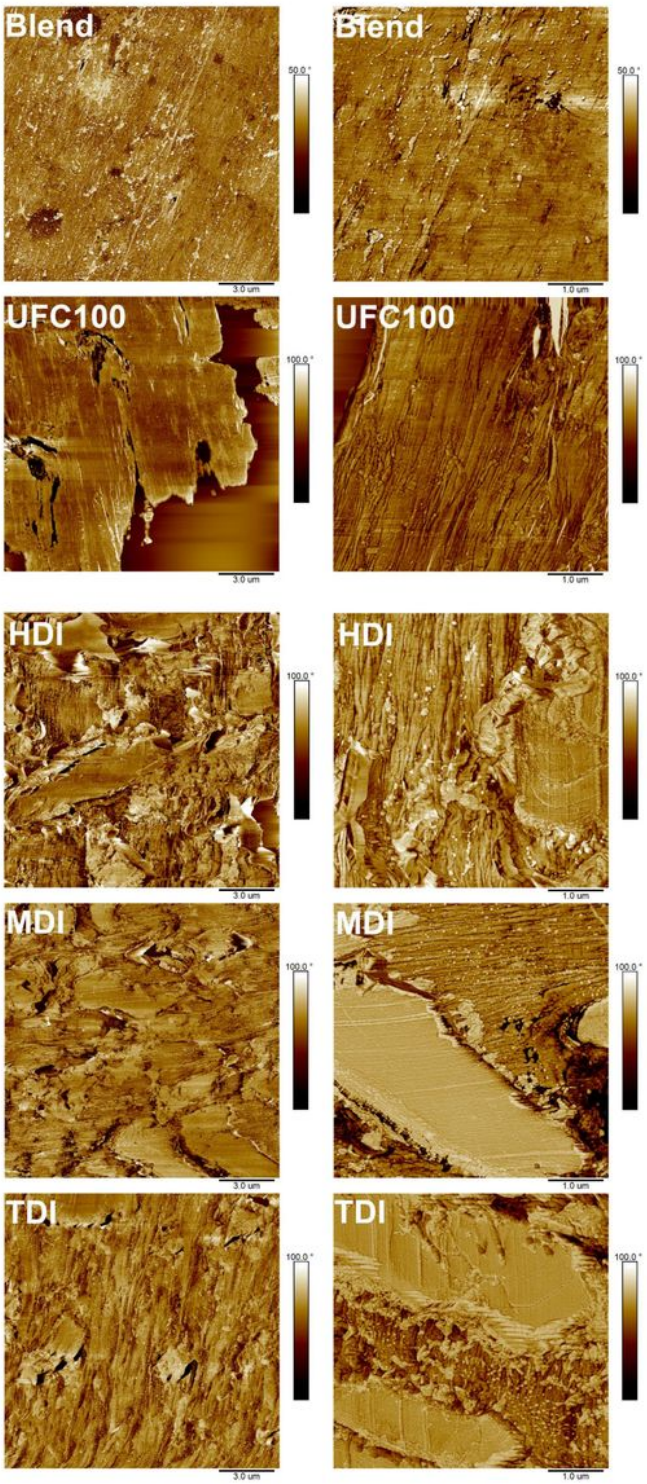

igure 10

FM phase images of the cross-sectional areas of studied samples.